Composites: Part B 43 (2012) 249–254

Contents lists available at SciVerse ScienceDirect

Composites: Part B

journal homepage: www.elsevier.com/locate/compositesb

A strain-gradient plasticity theory of bimodal nanocrystalline materials with composite structure

Yingguang Liu [a], Jianqiu Zhou [a,b,*], David Hui [c]

[a] Department of Mechanical Engineering, Nanjing University of Technology, Nanjing 210009, Jiangsu, People's Republic of China
[b] Department of Mechanical Engineering, Wuhan Institute of Technology, Wuhan 430070, Hubei, People's Republic of China
[c] Department of Mechanical Engineering, University of New Orleans, New Orleans, LA 70148, United States

ARTICLE INFO

Article history:
Received 17 March 2011
Accepted 28 November 2011
Available online 7 December 2011

Keywords:
A. Nano-structures
B. Mechanical properties
C. Analytical modelling

ABSTRACT

For the purpose of evaluating the mechanical property of bimodal nanocrystalline (nc) materials, a new composite constitutive model comprised of coarse grains evenly distributed in the nc matrix with respect to strain gradient has been developed. Due to their dissimilar properties and mismatch between the two phases, dislocation-controlling mechanism based on the statistically stored dislocations (SSDs) and geometrically necessary dislocations (GNDs) was analyzed and extended to consider the different influences of two parts in the composite model. We firstly built a stress–strain relation for strain gradient plasticity to predict the effect of grain size distribution on the flow stress. To describe the strain strength quantitatively, a strain-hardened law determined from strain gradient and a nanostructure characteristic length parameter were developed. The strain-hardened law and nanostructure characteristic length parameter were not the same as described in classical strain gradient theory.

1. Introduction

Even though exhibiting remarkable improvements in strength, most of the experimental studies reveal that nc materials generally possess insufficient ductility compared with their coarse-grained conventional counterparts [1,2]. However, the evidence of tensile superplasticity in nc materials has been reported, but these cases appear to be not numerous, and often occurring only at high temperatures, or with microtensile samples using specialized testing method [3–5].

As the deficiency of low ductility and the associated loss of toughness in some materials stop their applications in engineering. According to engineering practice and theoretical experience, people always build a composite structure to enhance the ductility of such materials [6–8]. Many approaches have been proposed to enhance the ductility of nc materials [9–12]. One of the several strategies that have been suggested for enhancing ductility in nc materials is to develop a bimodal grain size distribution, in which fine grains can provide high strength, whereas coarse grains can enable strain hardening to enhance ductility [13–15].

It can be seen from the above literatures that even though there are many experiment observations that the ductility of nc materials with a bimodal grain size distribution can be enhanced, there are few literatures doing quantitative study on the mechanical property of bimodal nc materials. Ovid'ko and Sheinerman [16] built a theoretical model that describes the generation of nanoscale cracks of bimodal nc materials, in the frame work of their model, cracks were generated in the stress field of interfacial disclination dipoles formed at the interfaces between larger grains and nc matrix during plastic deformation. But, it did not consider the constitutive relations. Fan et al. [17]. studied the plastic deformation and fracture of ultrafine-grained Al–Mg alloys with a bimodal grain size distribution, the Ramberg–Osgood equation was used to fit the compressive stress–strain curves of the bimodal ultrafine-grained (ufg) alloys, it was found that the plastic deformation of the ufg Al–Mg alloys with a bimodal microstructure was highly localized. The fracture of the alloys was attributed to shear localization under the compressive tests and to a combination of shear localization, cavitation and necking under the tensile tests. However, the grain size of their ufg matrix did not reach the nano-scale. Han et al. [18]. investigated the strain rate sensitivity and the strain rate effect on the ductility of 5083 bimodal alloys, the mechanical responses of several bimodal 5083 Al alloys with different fractions of coarse grains were studied at different strain rates. It was found that the failure strain increases with decreasing strain rate for the plastic deformation with strain rates less than $10^{-1}\ s^{-1}$, but it was very difficult to conduct quantitative calculation using their model. Besides, there are many other literatures to study the bimodal nc materials [19–21], and most of them

* Corresponding author at: Department of Mechanical Engineering, Nanjing University of Technology, Nanjing 210009, Jiangsu, People's Republic of China. Tel.: +86 25 83588706; fax: +86 25 83374190.

E-mail address: zhouj@njut.edu.cn (J. Zhou).

1359-8368/$ - see front matter © 2011 Elsevier Ltd. All rights reserved.
doi:10.1016/j.compositesb.2011.11.048

mainly described the experimental phenomena rather than established a constitutive model to take quantitative analysis.

In order to solve the above problems, a new composite constitutive model comprised of coarse grains evenly distributed in the nc matrices (as shown in Fig. 1) with respect to strain gradient has been developed. Due to their dissimilar properties and mismatch between the two phases, we treat it as a composite model. Dislocation-controlling mechanism based on the statistically stored dislocations (SSDs) and geometrically necessary dislocations (GNDs) was analyzed and extended to nc regime to consider the different influences of the two parts in the composite model, respectively. A stress–strain relation for strain gradient plasticity was firstly built to predict the effect of grain size distribution on the flow stress. In addition, a strain-hardened law determined from strain gradient and a nanostructure characteristic length parameter which differed from that of classical strain gradient theory was introduced in detail.

2. A strain gradient theoretical model for bimodal nc materials

The strain gradient near the interface, due to the different orientation and mismatch of neighboring grains, has been observed in several previous works [22–25]. Mitsuishi et al. [23] reported that the strain gradient was found during defect introduction processes in two differently sized Xe nanocrystals embedded in Al, the apparent displacements of Xe atom columns were observed with in situ high resolution electron microscopy and reduced from the middle Xe column to the Al matrix/Xe precipitate interface. The smaller value of shear displacement at the interface represents some compromise between the strain field of the partial dislocation and the requirement of compatibility resulting from the different elastic module and atoms arrangement of Al matrix and Xe nanocrystals precipitate.

Moreover, in order to exactly describe non-uniform plastic deformation associated with a size dependent effect, more current studies incorporate the strain gradient and internal length scale with conventional crystal plasticity model. For instance, in early 1970s, the gradient of plastic deformation in the microstructure has been introduced by Ashby and co-workers to analyze the stress–strain relationship influenced by grain sizes and dispersion of particles [26]. The earlier representative theory, mechanism-based theory of strain gradient plasticity (MSG), has been proposed by Gao et al. [27] based on a multi-scale framework linking SSDs and GNDs to the plastic flow stress and strain gradient through Taylor hardening expression

$$\tau_p = \alpha\mu b\sqrt{\rho_S + \rho_G}, \tag{1}$$

where τ_p, b, α and μ are the plasticity flow stress, Burgers vector, empirical constant and shear modulus, respectively. The total dislocation density is divided into the density of SSDs ρ_S and that of GNDs ρ_G. The concept of GNDs was introduced by Nye and Ashby to account for modes of plastic deformation, such as bending of a beam, where an internal accumulation of dislocations is required to accommodate the gradients of plastic strain induced by the deformation [28].

To further investigate the strain gradient effects on mechanical properties of nc materials, numerical studies confined attention to a single slip system of a single crystal in which a slip resistance g and a back stress τ_b exist. In Mitsutoshi's theory [29], a scale dependent crystal viscoplasticity model with a second strain gradient effect related to the second derivative of the plastic slip was introduced. The back stress is determined by spatial gradient of GNDs density ρ_G through

$$\tau_b = B\frac{\partial \rho_G}{\partial x_j}s_j, \tag{2}$$

where B denotes a back stress coefficient and s_j is the unit vectors specifying the slip direction. The GND density ρ_G is related to the spatial gradients in slip, which can be written in the form

$$\rho_G = \frac{\partial \gamma}{b\partial x_j}s_j, \tag{3}$$

where γ denotes a plastic slip and b denotes the magnitude of Burgers vector, respectively. Moreover, Ma et al. [30] and Evers et al. [31]. also developed their own mechanical model including GND and SSD on each slip system in order to consider strain gradients and additional hardening, the magnitude of which were related to grain size. Some articles [22,32] reported that the strain gradient was of high magnitude near the interfaces in nc materials due to the mismatch of neighboring grains with different orientations.

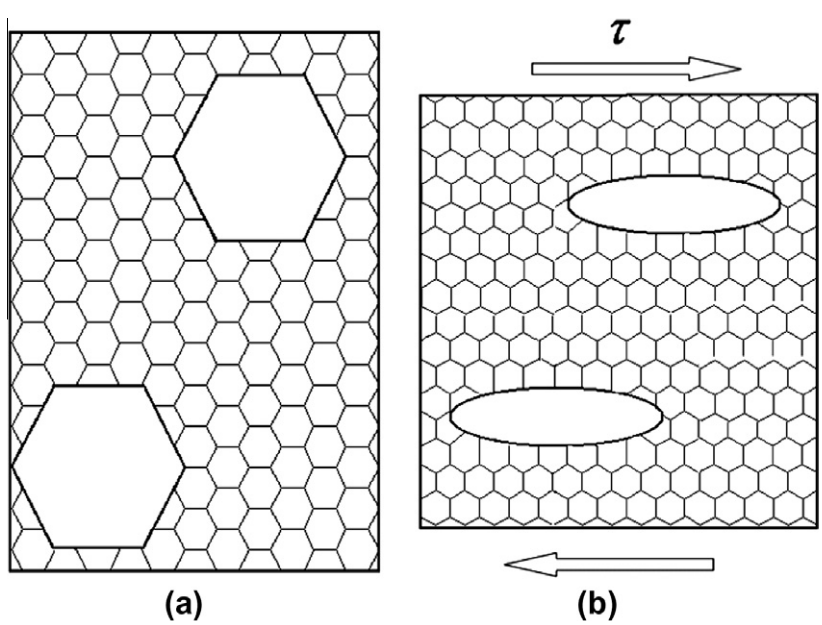

Fig. 1. View of (a) the generated bimodal microstructure and (b) the deformation of the coarse grains when under macroscopical load.

To analyze the overall mechanical behavior of nc materials realistically, the strain gradient effects should not be neglected. These theoretical frameworks as mentioned above have incorporated with the strain gradient, but not discussed deeply and quantified. They also did not take into account the difference in dislocation density observed between the grain interiors and the grain boundary (GB) regions. Furthermore, the strain gradient effects are responsible for the formation of strain hardening. Inspired by the above conclusions, in our present paper, to predict the grain size effects on bimodal nc materials analytically, a representative unit cell model is adopted as shown in Fig. 2, which is subjected to an applied shear stress τ. Here, the representative unit cell is a composite mechanical model consisting of a nano-grain and a coarse-grain. During plastic deformation process, there exist different deformation mechanisms in the two phases because of their dissimilar physical properties. Due to its extremely ordered atomic structure, the same oriented atom arrays and the high yield strength compared with coarse grains, the nano-grain is assumed to generate the uniform plastic deformation produced by the SSDs. An important reason for this assumption is to simplify the calculation and this assumption does not affect our results. Different from the perfect lattice in the nano-grain, various defects exist inside the coarse grains, so the coarse grain region is realized to develop nonhomogeneous plastic deformation with respect to GNDs and SSDs. Here the GNDs ensure compatibility of deformation and accommodate strain gradients in the case of nonhomogeneous deformation. At a given applied resolved shear stress, we assume that the coarse grain with a nonhomogeneous plastic strain γ_c and the nano-grain with a small uniform strain γ_n. Here we denote that the plastic strain of coarse grain near the nc matrices is identical with that of the nc grain, and the different strains are taken to be presented in the coarse grain, which increases gradually with increasing the distance from the nano-grain due to the dislocation based on slip processes. Both the dislocations within coarse grain and those within nano-grain contribute to the overall grain work hardening through Taylor's theory of the flow stress

$$\tau_p = \alpha\mu b\sqrt{\rho_T}. \quad (4)$$

Here, the total dislocation density is represented as a sum of the density of GNDs and the SSDs by a rule of mixtures, which can be obtained using the following equation

$$\rho_T = f_{coarse}(\rho_{SC} + \rho_G) + f_{nano}\rho_{SN}, \quad (5)$$

where f_{nano} and f_{coarse} are the volume fractions of the nc matrices and the coarse grains, ρ_{SC} and ρ_{SN} are density of SSDs in the coarse grains and nc matrices, respectively. According to Eq. (5), we can distinctly describe that the dislocations density within the coarse grains will play an increasing role in the whole dislocations density with the increasing f_{coarse}. By contrast, the contribution of the density within the nc matrices to the whole dislocations will gradually reduced.

2.1. Density of GNDs

Fig. 3 shows the idealized loops of GNDs traveling through the coarse grain, which are required for strain compatibility due to the mismatch between the two different phases. The geometrical mean strain gradient associated with GNDs within the coarse grain can be defined as

$$\eta = \frac{\gamma_c - \gamma_n}{\phi_1 d_{coarse}}, \quad (6)$$

where ϕ_1 is the geometrical factor. According to geometrical deformation condition as introduced in Figs. 2 and 3, we can describe the shear strain created by GNDs approximately by the following formula

$$\gamma_G = \gamma_c - \gamma_n = \frac{\phi_2 nb}{d_{coarse}}, \quad (7)$$

where n is the number of GNDs in a single coarse grain, ϕ_2 is the geometrical factor and b is the magnitude of Burgers vector. Thus, the average length of an idealized dislocation loop, for the sake of simplicity, is assumed to be equal to d_{coarse}. Therefore, the density of GNDs can be obtained by

$$\rho_G = \frac{n\lambda}{V} = \frac{3(\gamma_c - \gamma_n)}{4\pi\phi_2 d_{coarse} b}. \quad (8)$$

where λ is the average length of an idealized dislocation loop and V is deformed volume of dislocations evolution which is equal to the volume of the coarse grain.

2.2. Density of SSDs

In order to describe the constitutive behavior of the nc matrices in bimodal nc materials, a dislocation density-related unified constitutive model is used to determine the density of SSDs below. During the deformation process controlled by dislocation mechanism, the evolution of the SSDs density (ρ_S) is determined by

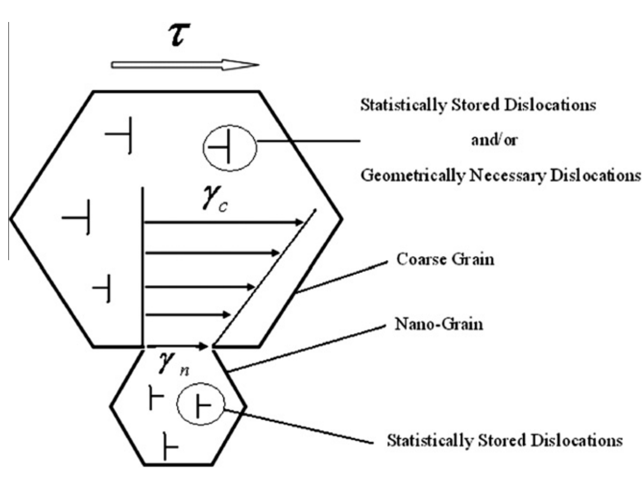

Fig. 2. Two-dimensional composite model undergoes plastic deformation.

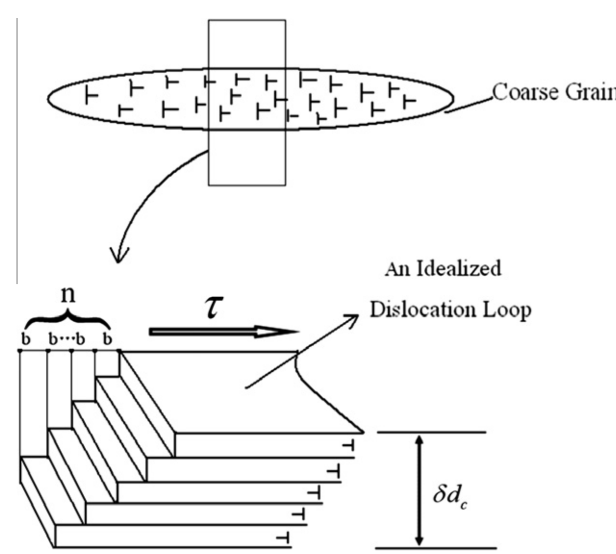

Fig. 3. Arrangement of GNDs within the coarse grain.

two dynamic processes: athermal storage of dislocations (ρ_S^+) and annihilation of dislocations (ρ_S^-). For a given overall strain (γ_n) dominated by dislocations within the nc grain, one can get

$$\rho_S(\gamma_n) = \rho_S^+(\gamma_n) + \rho_S^-(\gamma_n). \tag{9}$$

Capolungo et al. [32] proposed a model accounting for the athermal storage of dislocations based on the statistical approach derived by Kocks and Mecking [33]. Based on those models, the relation between ρ_S^+ and γ_n can be written as

$$\frac{d\rho_S^+}{d\gamma_n} = \frac{M}{b}\left(\frac{1}{d_n} + \xi\sqrt{\rho_S}\right), \tag{10}$$

where M, b, d_n and ξ are the Taylor orientation factor, Burgers vector, size of the nc grain and proportionality factor, respectively; and the dynamic recovery process controlled by the annihilation of stored dislocations is described by

$$\frac{d\rho_S^-}{d\gamma_n} = -C_{20}\left(\frac{\dot{\gamma}_n}{\dot{\gamma}_0}\right)^{-1/m} \cdot \rho_S, \tag{11}$$

where C_{20} and $\dot{\gamma}_0$ are constant, and m is inversely proportional to the temperature T.Combining Eqs. (10) and (11), the evolution of dislocation density with the increasing of γ_n can be obtained as follows

$$\frac{d\rho_S}{d\gamma_n} = \frac{d\rho_S^+}{d\gamma_n} + \frac{d\rho_S^-}{d\gamma_n} = \frac{M}{b}\left(\frac{1}{d_n} + \xi\sqrt{\rho_S}\right) - C_{20}\left(\frac{\dot{\gamma}_n}{\dot{\gamma}_0}\right)^{-1/m} \cdot \rho_S. \tag{12}$$

Employing the relation $\sigma_p = M\tau_p$, where M is the Taylor orientation factor, and substitution of Eqs. (8) and (9) into Eq. (4) leads to the plastic flow stress–strain relation related to gradient dependent on GNDs

$$\sigma_p = M\alpha\mu b\sqrt{f_{nano}\rho_{SN} + f_{coarse}\rho_{SC}}. \tag{13}$$

Furthermore, considering synthetically the elastic stage of deformation and plastic stage due to two different kinds of dislocations, the total constitutive relationship of the representative unit for a given applied stress is then given by

$$\sigma = \sigma_e + \sigma_p. \tag{14}$$

where σ_e is an elastic deformation term.

3. Results and discussion

3.1. Stress/strain responses

To understand the mechanical property of bimodal nc materials, numerical simulations based on the aforementioned model were carried out for the cases of copper. The bimodal microstructure consisting of coarse grains (grain sizes f_{coarse} = 2 μm) evenly distributed in the nc matrices (average grain sizes d_{nano} = 50 nm). The deformation behavior under uniaxial tension was investigated. Detailed information about the parameters of nc Cu are listed in Table 1 [34].

Table 1
Material parameters in calculation for Cu.

Description	Notation	Value
Empirical constant	α	0.2–0.5
Magnitude of the burgers vector	b	0.256×10^{-9} m
Shear modulus of copper	μ	42.1 GPa
Taylor orientation factor	M	3.06
Proportionality factor	ξ	0.2
Numerical constant	C_{20}	18.5
Numerical constant	m	12.5
Geometrical factor	ϕ_1	0.2–0.5
Geometrical factor	ϕ_2	0.5–1
Reference strain rate	$\dot{\gamma}_0$	1 s^{-1}

The stress–strain curves obtained from the present model are displayed as a function of coarse grain (CG) content in Fig. 4. It can be seen that the developed model seems to have captured the flow stress level, work hardening features. Inspection of Fig. 4 reveals that the yield strength decreases with increasing the CG content, and the ductility increases with increasing the CG content. e.g. When the volume fraction of coarse grains increases from 10% to 30%, the ductility and toughness of the sample increases nearly 70%, while the yield stress decreases only 14%. In addition, all the stress–strain curves show continuous strain hardening, and the work-hardening region increases with increasing the CG content. These phenomenons are consistent with the uniaxial tension stress–strain behavior reported for bimodal nc materials, which show that because of the larger grain size and fewer obstacles to slip, dislocations glide more easily in the coarse-grained regions than in the nanostructured regions, so, coarse grains can enable strain hardening to enhance ductility. In terms of load transfer, the nc matrix sustain most of the applied stress and only a small part of the load is transferred to the softer coarse grains, and this produces a slight decrease in yield strength. In addition, stress concentrations in the nc matrix may be relaxed by transferring local loads to the softer coarse-grained regions [35]. Further more, it can be noted from Fig. 4 that the strain hardening increases with the increasing CG content. As we know, for nc material, strain hardening is mainly due to the dislocation pile-ups along grain boundary regions, and the lack of strain hardening in nc materials is attributed to the lack of dislocation accumulation due to either small grain size or near-saturated dislocation density prior to mechanical testing [36–40]. Fig. 5 shows the strain dependence of ratio of GNDs density to total dislocations density calculated from our model. It can be found that the ratio increases with increasing the CG content, e.g. the ratio with 30% CG increased nearly 300% compared with the 10% CG sample under the strain of 10%. From the above analysis we can see that in the bimodal nc materials, fine grains are responsible for the strain hardening rate sensitivity, whereas coarse grains can enable strain hardening to enhance ductility.

3.2. Strain hardening description

As we know, the work hardening of alloys is much faster than pure single crystals, because their two or more nonhomogeneous

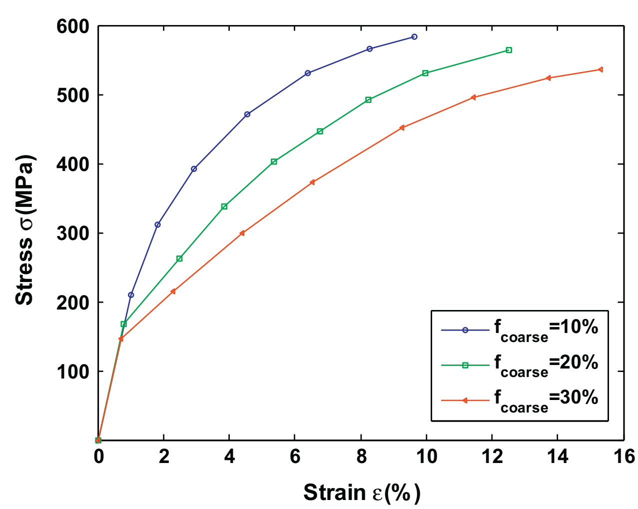

Fig. 4. The calculated stress–strain relations (under uniaxial tension) for bimodal nc Cu with different CG contents.

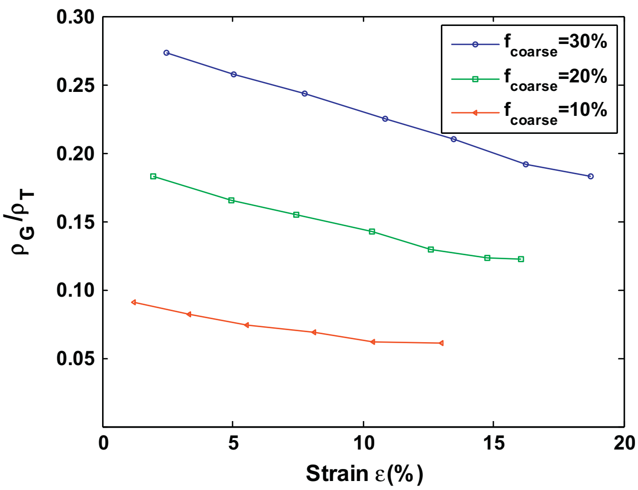

Fig. 5. Ratio of GNDs density to total dislocations density increases with increasing coarse grain content calculated from our model.

phases do not deform equally. From many previous results, it is now generally recognized that the inherent anisotropy of crystal lattice is expected to become increasingly significant with the decreasing grain size scale, especially for bimodal nc materials consisting of two phases with different physical properties: the plastically softer coarse phase and regular nc matrix. In general, the non-uniform deformation of coarse grains has a significant effect on the mechanical response of nanocrystals. In order to exactly describe the overall constitutive relationship, the effects of strain gradient between coarse grains and nc matrix cannot be neglected. Here, we assume the SSDs with respect to compatibility of deformation between nc matrix and coarse grains contribute directly to the work hardening. The plastic flow stress generated by SSDs can be described as

$$\sigma_m = M\alpha\mu b\sqrt{f_{nano}\rho_{SN} + f_{coarse}\rho_{SC}}. \tag{15}$$

According to the calculation of stress–strain relation in Section 3.1, we can get a strain-hardened law dependent on gradient

$$\left(\frac{\sigma_p}{\sigma_m}\right)^2 = 1 + f_{coarse}\left(\frac{3\phi_1 M^2\alpha^2\mu^2 b}{4\pi\phi_2\sigma_m} - 1\right)\eta. \tag{16}$$

Obviously, the expression $(M^2\alpha^2\mu^2 b)/\sigma_m$ has been considered as an intrinsic length scale l in many literatures [41,42]. The length scale parameter plays a significant role in gradient plasticity of the micrometer range. It can be observed in numerous experiments that down-scaling of the specimen dimensions leads to deviations in the mechanical responses of materials once at least one of the dimensions becomes comparable with intrinsic material length scale parameter [42] In a recent study [43], the length scale l was predicated to be a variable depending on the deformation history and other various parameters including the grain size, the characteristic dimension of the specimen and so on. In order to obtain one more general hardening relation, Eq. (16) is reestablished to be

$$\sigma_p = \sqrt{1 + f_{coarse}\left(\frac{3\phi_1 M^2\alpha^2\mu^2 b}{4\pi\phi_2\sigma_m} - 1\right)\eta} \cdot \sigma_m. \tag{17}$$

We take all the parameters before η in Eq. (17) to be one variable $\hat{l}$, a nanostructure characteristic length parameter. Thus, employing the relation

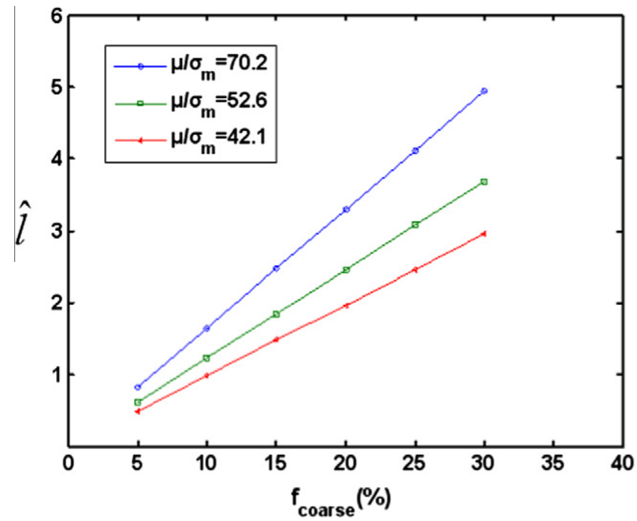

Fig. 6. Variation of nanostructure characteristic length parameter $\hat{l}$ with f_{coarse} under three different deformation conditions.

$$\hat{l} = f_{coarse}\left(\frac{3\phi_1 M^2\alpha^2\mu^2 b}{4\pi\phi_2\sigma_m} - 1\right), \tag{18}$$

we can get

$$\sigma_p = \sigma_m\sqrt{1 + \hat{l}\eta}. \tag{19}$$

Most importantly, nanostructure characteristic length parameter $\hat{l}$ here is not a material constant but associated with grain size of the nc matrix and volume friction of coarse grains f_c. To be noted that the larger $\hat{l}$ is, the stronger effect of deformation hardening is. It is obviously found from Eq. (19) that the magnitude of strain hardening of bimodal nc materials is determined by both the characteristic length parameter $\hat{l}$ and strain gradient η. This is mainly because of the existence of mismatch between the coarse grains and the nc matrices which results in the emergence of strain gradient. In order to show quantitatively the effect of strength, here the variation of nanostructure characteristic length parameter $\hat{l}$ with volume fraction of coarse grains f_{coarse} is shown in Fig. 6. To be noted that in Fig. 6, for all the curves, the value of $\hat{l}$ increases linearly as f_{coarse} decreases. This feature of the curves just indicates that the coarse grains have higher strain hardening capability than the nc grains.

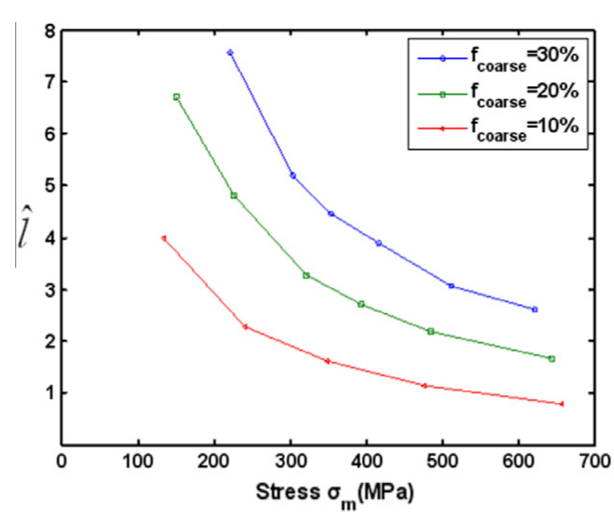

Fig. 7. Variation of nanostructure characteristic length parameter $\hat{l}$ with σ_m at three different CG contents.

In addition, the feature of $\hat{l}$ as shown in Fig. 7 precisely describes the work hardening capacity during the deformation process with different CG content. The visible reduction of $\hat{l}$ can be seen as σ_m increases, which denotes that the strain hardening becomes increasingly more difficult with the continuous increasing strain deformation and tends toward constant gradually.

4. Conclusion

To systematically understand the effect of grain size, grain size distribution on the mechanical response of bimodal nc materials, A strain-gradient plasticity theory of bimodal nc materials based on dislocation density has been developed. Due to their dissimilar properties and mismatch between the two phases, dislocation-controlling mechanism based on the SSDs and GNDs was analyzed and extended to consider the different influences of two parts in the composite model. A stress–strain relation for strain gradient plasticity was firstly built to predict the effect of grain size distribution on the flow stress. A strain-hardened law determined from strain gradient and a nanostructure characteristic length parameter which differed from that of classical strain gradient theory were also introduced.

Based on the numerical simulations, we obtained some conclusions as following:

- Nc materials with a bimodal structure exhibit a combination of high strength and good ductility. In this sort of materials, fine grains provide high strength, whereas coarse grains can enable strain hardening to enhance ductility.
- As the volume fraction of coarse grains increased, tensile ductility increased and strength decreased.
- Coarse grains have higher strain hardening capability than the nc grains, and continuous strain hardening increases with increasing the CG content.
- Coarse grains have higher strain hardening capability than the nc grains and the strain hardening becomes increasingly more difficult with the continuous increasing strain deformation and tends toward constant gradually.
- Strain gradient in bimodal nc materials contributes directly to the mechanical behaviors of this sort of materials and cannot be neglected.

Acknowledgements

The authors are grateful for the funding of the National Natural Science Foundation of China (10502025, 10872087), Fok Ying Tong Education Foundation (101005), and Natural Science Foundation of Jiangsu Province (BK2007528).

References

[1] Koch CC, Morris DG, Lu K, Inoue A. Ductility of nanostructured materials. MRS Bull 1999;24:54–8.
[2] Kumar KS, Swygenhoven V, Suresh S. Mechanical behavior of nanocrystalline metals and alloys. Acta Mater 2003;51:5743–74.
[3] Zhang S, Wang H, Scattergood RO, Narayan J, Koch CC, Sergueeva AV, et al. Tensile elongation (110%) observed in ultra-fine-grained Zn at room temperature. Appl Phys Lett 2002;81:823–5.
[4] Karimpoor AA, Erb U, Aust KT, Palumbo G. High strength nanocrystalline cobalt with high tensile ductility. Scripta Mater 2003;49:651–6.
[5] Valiev RZ, Alexandrov IV, Zhu YT, Lowe TC. Paradox of strength and ductility in metals processed by severe plastic deformation. J Mater Res 2002;17:5–8.
[6] Pasto AE, Braski DN, Watkins TR, Porter WD, Lara-Curzio E, McSpadden SB. Characterization techniques for composites and other advanced materials. Composites: Part B 1999;30:631–46.
[7] Cao GX, Chen X, Xu ZH, Li XD. Measuring mechanical properties of micro- and nano-fibers embedded in an elastic substrate: theoretical framework and experiment. Composites Part B 2010;41:33–41.
[8] Neralla S, Kumar D, Yarmolenko S, Sankar J. Mechanical properties of nanocomposite metal–ceramic thin films. Composites: Part B 2004;35:157–62.
[9] Dao M, Lu L, Asaro RJ, Hosson JTMD, Ma E. Toward a quantitative understanding of mechanical behavior of nanocrystalline metals. Acta Mater 2007;55:4041–65.
[10] Zhang X, Wang H, Koch CC. Mechanical behavior of bulk nanocrystalline Zn. Rev Adv Mater Sci 2004;6:53–99.
[11] Han BQ, Lavernia E, Mohamed FA. Mechanical properties of nanostructured materials. Rev Adv Mater Sci 2005;9:1–16.
[12] Ovid'ko IA. Superplasticity and ductility of superstrong nanomaterials. Rev Adv Mater Sci 2005;10:89–104.
[13] Wang Y, Chen M, Zhou F, Ma E. High tensile ductility in a nanostructured. Metal Nature 2002;419:912–5.
[14] Wang YM, Ma E, Chen MW. Enhanced tensile ductility in nanostructured Cu. Appl Phys Lett 2002;80:2395–7.
[15] Chokshi AH, Mukherjee AK. A topological study of superplastic deformation in an Al–Li alloy with a bimodal grain size distribution. Metall Trans A 1988;19:1621–4.
[16] Ovid'ko IA, Sheinerman AG. Plastic deformation and fracture processes in metallic and ceramic nanomaterials with bimodal structures. Rev Adv Mater Sci 2007;16:1–9.
[17] Fan GJ, Choo H, Liaw PK, Lavernia EJ. Plastic deformation and fracture of ultrafine-grained Al–Mg alloys with a bimodal grain size distribution. Acta Mater 2006;54:1759–66.
[18] Han BQ, Huang JY, Zhu YT, Lavernia EJ. Strain rate dependence of properties of cryomilled bimodal 5083 Al alloys. Acta Mater 2006;54:3015–24.
[19] Han BQ, Lee Z, Witkin D, Nutt S, Laveravi EJ. Deformation behavior of bimodal nanostructured 5083 Al alloys. Metall Mater Trans A 2005;36:957–65.
[20] Prasad MJNV, Suwas S, Chokshi AH. Microstructural evolution and mechanical characteristics in nanocrystalline nickel with a bimodal grain-size distribution. Mater Sci Eng A 2009;503:86–91.
[21] Lee Z, Witkin DB, Radmilovic V, Lavernia EJ, Nutt SR. Bimodal microstructure and deformation of cryomilled bulk nanocrystalline Al–7.5Mg alloy. Mater Sci Eng A 2005;410:462–7.
[22] Ke M, Hackney SA, Milligan WW, Aifantis EC. Observation and measurement of grain rotation and plastic strain in nanostructured metal thin films. Nanostruct Mater 1995;5:689–97.
[23] Mitsuishi K, Song M, Furuya K, Birtcher RC. Observation of atomic processes in Xe nanocrystals embedded in Al under 1 MeV electron irradiation. Nucl Instrum Methods Phys Res B 1999;148:184–8.
[24] Shu JY, Fleck NA. Strain gradient crystal plasticity: size-dependent deformation of bicrystals. J Mech Phys Solids 1999;47:297–324.
[25] Wang GF, Feng XQ, Yu SW, Nan CW. Interface effects on effective elastic moduli of nanocrystalline materials. Mater Sci Eng A 2003;363:1–8.
[26] Ashby MF. The deformation of plastically non-homogeneous alloys. Phil Magn 1970;21:399–424.
[27] Gao H, Huang Y, Nix WD, Hutchinson JW. Mechanism-based strain gradient plasticity—I. Theory. J Mech Phys Solids 1999;47:1239–63.
[28] Needleman A, Van der Giessen E. GNDs in nonlocal plasticity theories: lessons from discrete dislocation simulations. Scripta Mater 2003;48:127–32.
[29] Kitsutoshi M, Tiggo V. Studies of scale dependent crystal viscoplasticity models. J Mech Phys Solids 2006;54:1789–810.
[30] Ma A, Roters F, Raabe D. A dislocation density based constitutive model for crystal plasticity FEM including geometrically necessary dislocations. Acta Mater 2006;54:2169–79.
[31] Evers LP, Parks DM, Brekelmans WAM, Geers MGD. Crystal plasticity model with enhanced hardening by geometrically necessary dislocation accumulation. J Mech Phys Solids 2002;50:2403–24.
[32] Capolungo L, Jochum C, Cherkaoui M, Qu J. Homogenization method for strength and inelastic behavior of nanocrystalline materials. Int J Plasticity 2005;2:67–82.
[33] Kocks UF, Mecking H. Physics and phenomenology of strain hardening: the FCC case. Prog Mater Sci 2003;48:171–273.
[34] Liu YG, Zhou JQ, Ling X. Impact of grain size distribution on the multiscale mechanical behavior of nanocrystalline materials. Mater Sci Eng A 2010;527:1719–29.
[35] Lee Z, Nutt SR, Rodriguez R, Hayes RW, Lavernia EJ. Microstructural evolution and deformation of cryomilled nanocrystalline Al–Ti–Cu alloy. Metall Mater Trans A 2003;34:1473–81.
[36] Jain M, Christman T. Synthesis, processing, and deformation of bulk nanophase Fe–28Al–2Cr intermetallic. Acta Metall 1994;42:1901–11.
[37] Carsley JE, Fisher A, Milligan WW, Aifantis EC. Mechanical behavior of a bulk nanostructured iron alloy. Metall Mater Trans A 1998;29A:2261–71.
[38] Jia D, Ramesh KT, Ma E. Effects of nanocrystalline and ultrafine grain sizes on constitutive behavior and shear bands in iron. Acta Mater 2003;51:3495–509.
[39] Semiatin SL, Jata KV, Uchic MD, Berbon PB, Matejezyk DE, Bampton CC. Plastic flow and fracture behavior of an Al–Ti–Cu nanocomposite. Scripta Mater 2001;44:395–400.
[40] Han BQ, Lavernia EJ, Mohamed FA. On the mechanical behavior of a cryomilled Al–Ti–Cu alloy. Mater Sci Eng A 2003;358:318–23.
[41] Han CS, Gao H, Huang Y, Nix WD. Mechanism-based strain gradient crystal plasticity—I. Theory. J Mech Phys Solids 2005;53:1188–203.
[42] Estrin Y, Molotnikov A, Davies CHJ, Lapovok R. Strain gradient plasticity modelling of high-pressure torsion. J Mech Phys Solids 2008;56:1186–202.
[43] Al-Rub RKA, Voyiadjis GZ. A physically based gradient plasticity theory. Int J Plasticity 2006;22:654–84.